IMPACTS OF RADIANCE ASSIMILATION IN THE JMA OPERATIONAL MESO-SCALE ANALYSES AND FORECASTS

Masahiro Kazumori

Japan Meteorological Agency, 1-3-4 Otemachi Chiyoda-ku, Tokyo, Japan

Abstract

This paper describes the operational implementation of radiance assimilation in JMA operational meso-scale analysis system. RTTOV was introduced into the JMA non-hydrostatic model variational data assimilation (JNoVA) system as a satellite radiance observation operator. Clear sky radiances are assimilated in the initial implementation. The radiance assimilation scheme was tested with the operationally available satellite radiance data such as AMSR-E, TMI, SSMIS, AMSU-A/B, MHS and MTSAT data. In this test, temperature retrievals from ATOVS and Total Column Water Vapour (TCWV) retrievals from microwave imagers, which had been used in JNoVA operation, were not used. A quality control of the radiance data used in JMA global analysis was applied for the meso-scale analysis. Several modifications on the treatment of the lower model top of the meso-scale model in the radiative transfer calculation and the data thinning distance for the high resolution meso-scale model were applied. The bias correction coefficients, which were determined in a variational bias correction scheme in the JMA global analysis, were applied. The radiance assimilation brought considerable improvements in the tropospheric analyses of temperature, humidity and also in the short-range forecasts. The improvements were ensured by the evaluation with radiosonde observations. Assimilations of the radiances from various microwave imagers and humidity sounders produced similar TCWV analysis increment to those of the retrieved TCWV assimilation around Japan Islands. Because radiance assimilation enables to use satellite data with no retrieval process, DMSP F-16 and F-17 SSMIS radiances were newly incorporated. The data brought much moisture analysis increment over the ocean and strengthened the contrast between moist and dry area in a typhoon event. Simulated MTSAT infrared image from the JNoVA analysis with the radiance assimilation showed similar features to the real MTSAT infrared image. Better precipitation forecast was confirmed in the verification with the rainfall product from ground-based radars and rain gauges in Japan. Based on those findings, the radiance assimilation scheme was implemented in the JMA operational meso-scale NWP system on 13 December 2010.

INTRODUCTION

Japan Meteorological Agency (JMA) operates a regional numerical weather prediction model, which is called Meso-Scale Model (MSM). The main objective of JMA's MSM is to provide guidance for issuing warnings and very short-range forecasts of precipitation covering Japan and its surrounding areas. Because Japan is an island country surrounded by the ocean, moisture information over the ocean is one of the key issues for the accurate precipitation forecasting. Figure 1 shows the MSM domain and topography. The model's horizontal resolution is 5km and the mode top height is 21,800m with 50 vertical layers. The model is being operated eight times a day to produce the forecasts up to 33 hours from 03, 09, 15 and 21UTC Initial fields or 15 hours from 00, 06, 12 and 18UTC initial fields. The initial conditions of the MSM are produced by JMA non-hydrostatic model based variational data assimilation system (Honda et al., 2005). The meso-scale analysis uses a four dimensional variational assimilation scheme and it is performed every three hour. The assimilation time window is three hours and the observations delivered within 50 minutes after the analysis time are used operationally. As for in situ observations (i.e. conventional observations), surface pressure observations from weather stations, ships and buoys, radiosonde sounding observations, upper air temperature and wind data from aircraft observations and wind profilers' data are assimilated. Derived relative humidity data and doppler wind data from ground-based radar observations, pseudo observation of typhoon bogus are

also assimilated. Figure 2 shows a comparison of the day-time and night-time data coverages. Upper air sounding data with radiosonde observations are available in so-called synoptic times (0000, and 1200UTC).Less aircraft data are avaiable in night-time. In general, the conventinal observations are made predominantly during day-time. And the ocean is an observational data sparse area. This inhomogeneous data coverage in the three hourly analysis cycle and the imbalanced geographical distribution of in situ data between land and sea cause unstable analysis accuracy because the conventional obervations have still dominant effect in JMA meso-scale analysis system.

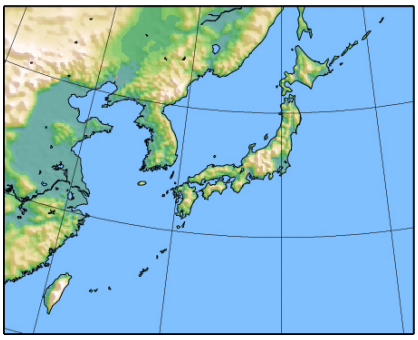

Figure 1: **MSM domain and topography**

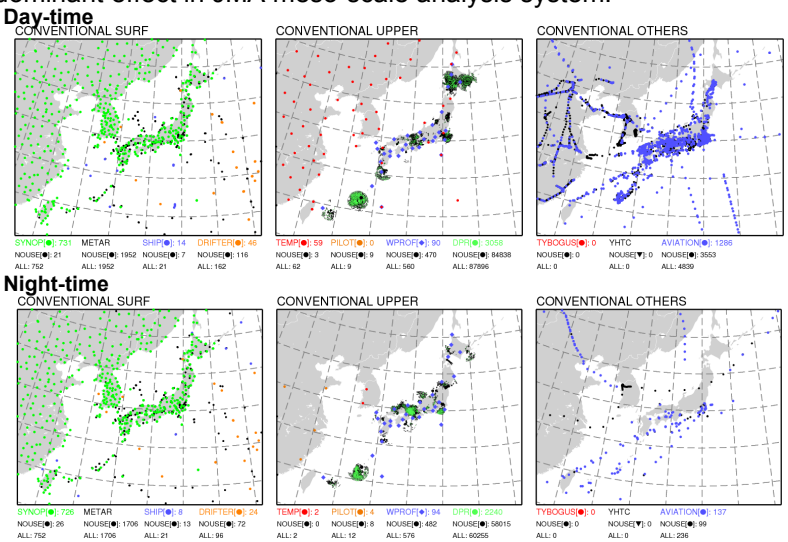

Figure 2: **Comparison of available conventional observation coverage in MSM. Upper panels indicate examples of 03 UTC coverage (day-time), and lower panels indicate those of 21 UTC (night-time). The left panels indicate surface observation from weather stations, ships and bouys. The middle panels indicate radiosonde observation, wind and relative humidity data derived from radar observations and wind profiler data. The right panels indicate airfract observations.**

As for space-based remote sensing observations, atmospheric motion vectors (AMV) derived from geostatinary satellite images, GPS Total Column Water Vapour (TCWV), rain rate derived from radar data and microwave imager data, and temperature and humidity information from various polar orbitting satellites and geostationaly sattelite (MTSAT) are available for the analysis.

TCWV and rain rate data derived from AMSR-E, TMI and temperature profiles derived from ATOVS instruments had been assimilated together with the other observation data. However, the retrieval assimilation is not suitable from operational point of view. Retrieval of geophysical parameters requires algorithms, which was that optimized for each instrument and geophysical quantity. It is likely to take time to develop the retrieval algorithm and release the products after satellite launch. Moreover, retrieval errors are complicated generally to understand and specify correctly in the data assimilation. And the unclear error contamination is unfavourable in the data assimilation. In contrast, the errors of the radiance observations are much simpler to describe the characteristics. And the radiance data include information over deep atmospheric layers which characterized by the weighing function in the radiative transfer model. Radiance assimilation enables us to assimilate that original information as it is.

Figure 3 shows comparisons of available satellite observation between retrieval assimilation and radiance assimilation. Left panels indicate the data coverages in the retrieval assimilation and right panels indicate those of the radiance assimilation. Usually, retrieved temperature profile data were delivered only clear scene because the products have good quality in the clear sky condition. However, radiance data which are sensitive to the higher atmospheric levels (upper troposphere and lower stratosphere) are also beneficial under cloudy condition. Radiance assimilation increase the data coverage even in a single sensor case. Clear sky radiance data (not affected by cloud and rain) from AMSU-A onboard NOAA 15, 16, 18, 19, Aqua and Metop, MHS onboard NOAA 18, 19 and Metop, MTSAT are assimilated in the system. We continue to use TCWV from ground-based GPS, rain rate retrieval from radar and microwave imagers. Rain rate from F-16, F-17 SSMIS were newly added in the system.

High frequent observations (i.e. MTSAT data, GPS TCWV, rain rate from radar) are also available for all analysis time. Although a polar obiting satellite visits only twice a day in MSM model domain, multiple satellites use in the analysis makes it possible to fill the gaps. Recently, most operational NWP centres use observed radiances directly in their global variational data assimilation system. For the forward and adjoint calculation in the variational data assimilation, fast radiative transfer model is necessary. We adopted RTTOV-9.3 (Sounders 2008) as the radiative transfer model which is used in JMA global analysis (Kazumori 2009a).

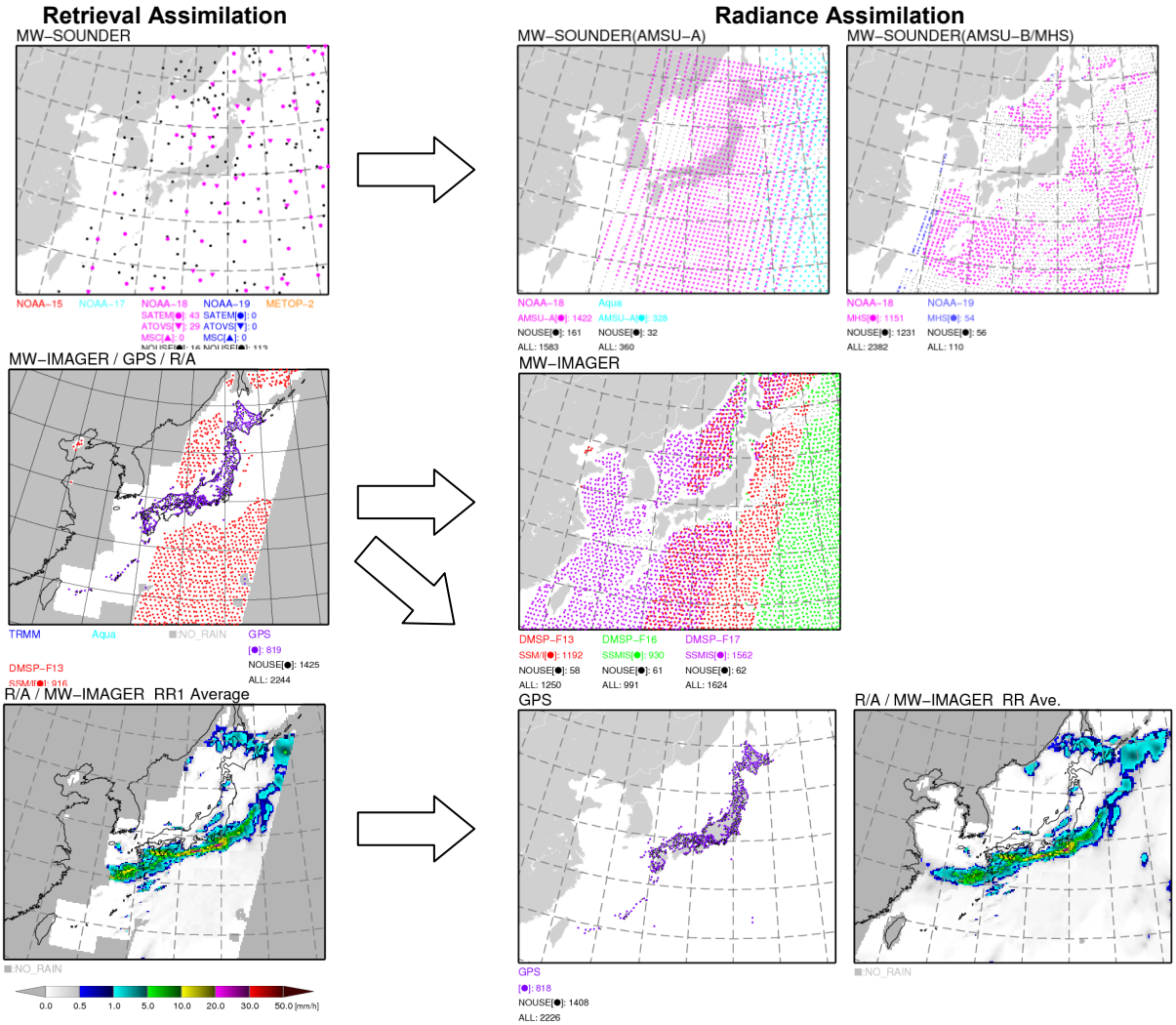

Figure 3: **Comparison of available remote sensing observation coverage in MSM. Left half panels indicate an example of the coverage in retreival assimilation. Top is for ATOVS temperature retrieval profiles, middle is for TCWV from microwave imager and GPS, bottom is for rain rate from radars and microwave imagers. Right half panels are for that of the radiance assimilation. Top and middle panels are for brightness temperatures and lower panes is for GPS TCWV and rain rate from radars and microwave imagers. The coverage of GPS TCWV was separately displayed in the radiance assimilation case.**

Basically, quality control of observation data is same with a method used in JMA global data assimilation (JMA 2007, Kazumori 2009b). Differences of MSM and JMA global model, however, require some modifications on the radiance data assimilation for meso-scale analysis from the configuration of JMA global data assimilation.

The one is data thinning distance. In JMA global data assimilation, the optimized data thinning distances from 180 to 250km are configured for each instrument. The inner model resolution of the global data assimilation is about 80km and that of the meso-scale data assimilation is 15km. In the first implementation of radiance assimilation scheme for MSM, 45km thinning distance was selected for all radiance data. It is clear that there is room for tuning of the data thinning distance.

The other is a treatment of the atmospheric profiles for the radiative transfer calculation. The global model top height is about 0.1 hPa and it covers necessary atmospheric profile for the radiative transfer calculation but MSM top height is about 40hPa and it is not sufficient for the calculation. The temperature profile over MSM top height is extrapolated from MSM model top temperature with U.S. standard atmosphere's lapse rate. Climatology of moisture and ozone profiles is employed for the upper air profiles. The use of extrapolated upper air atmospheric profiles (mostly over 40hPa) causes inaccurate radiative transfer calculation results for stratospheric sensitive channels.Figure 4 shows comparisons of AMSU-A brightness temperature's O-B (observed – background). The histograms showed similar feature for JMA global model and MSM in the channels 4-8. But the error of channel 9 in MSM is much larger than the global model. Also biases in averaged O-B horizontal distribution for channel 9 were found. Therefore, AMSU-A data from channel 4 to 8 were selected for the operational data assimilation.

The last important modification point is radiance bias correction. In the global data assimilation, two step bias corrections are applied. The first step is a correction of scan position dependent biases with static value. The second one is a variational bias correction by using a linear function with some predictors. The coefficients are optimized in the global analysis and updated every six hour. For the radiance bias correction in MSM analysis, the latest coefficients determined in the global analysis are employed with the same predictors calculated from MSM field. We assume that biases of atmospheric profiles and surface variables are small or similar characteristics between the global model and MSM. Actually, it is confirmed that the use of the coefficients with MSM's predictors work well in the radiance bias correction in MSM analysis. Further, the coefficients determined in the global analysis are more stable because the used data set for coefficient determination is global data and it covers various meteorological conditions although MSM analysis covers only limited area in temporally and spatially.

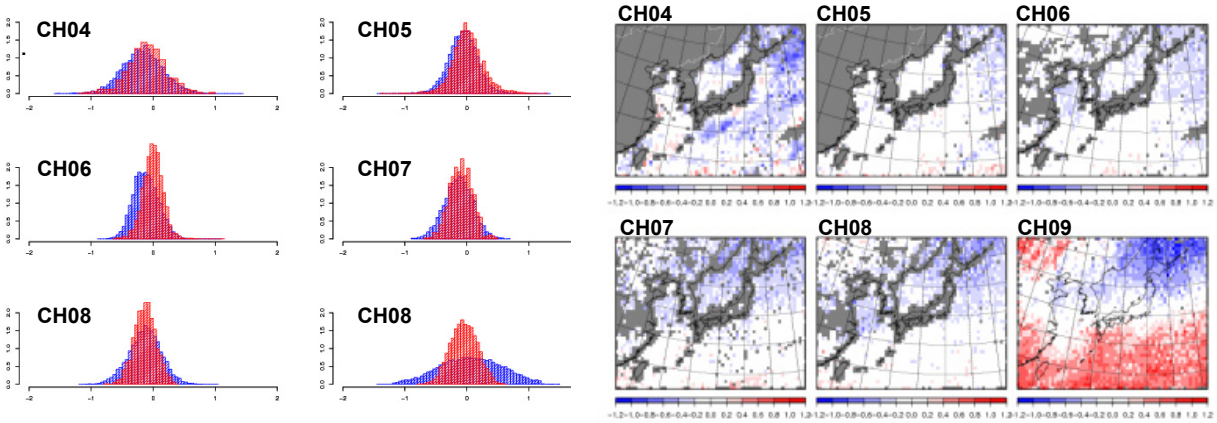

Figure 4: **Comparison of AMSU-A brightness temperature's O-B (observed – background). Left panels' histogram indicate frequency distribution of AMSU-A O-B for each channel in October 2009. Blue histgrams are for MSM and red histograms are for JMA global model. Right panels' indicate monthly mean of horizontal distribtuion AMSU-A O-B for each channel during the same period.**

ASSIMILATION EXPERIMENTS

In order to investigate the impacts of direct radiance assimilation for JMA operational meso-scale analyses and forecasts, several assimilation experiments were performed. In this paper, verification result of RMSE of geopotential height forecast against radiosonde observations and two case studies were selected to show the impacts. In Test run, radiance data from Microwave Imagers (AMSR-E, TMI) and Microwave Sounders (AMSU-A) were assimilated instead of those retrievals. In addition, radiance data from DMSP F-16, F-17 SSMIS, NOAA-18, -19, Metop MHS and MTSAT Clear Sky Radiance (CSR) were also incorporated. In Control run, the temperature retrieval from ATOVS and Total Column Water Vapour from Microwave Imagers were assimilated in the same way as JMA operational meso-scale NWP system as of November 2010. Rain rate retrievals from Microwave Imagers were assimilated in the both experiments and F-16, F-17 SSMIS's rain rate retrievals were newly added in Test run. Usage of other observation data was same in both run. We perform three hourly assimilation cycles and ran MSM to produced 33 hours forecasts from 03, 09, 15 and 21UTC

Initial fields. The periods of the assimilation experiments were 00TUC July 15 -21UTC July, 2009, 00UTC July 1 – 21UTC July 5, 2010, and 00UTC August 9 – 21UTC August 12, 2010.

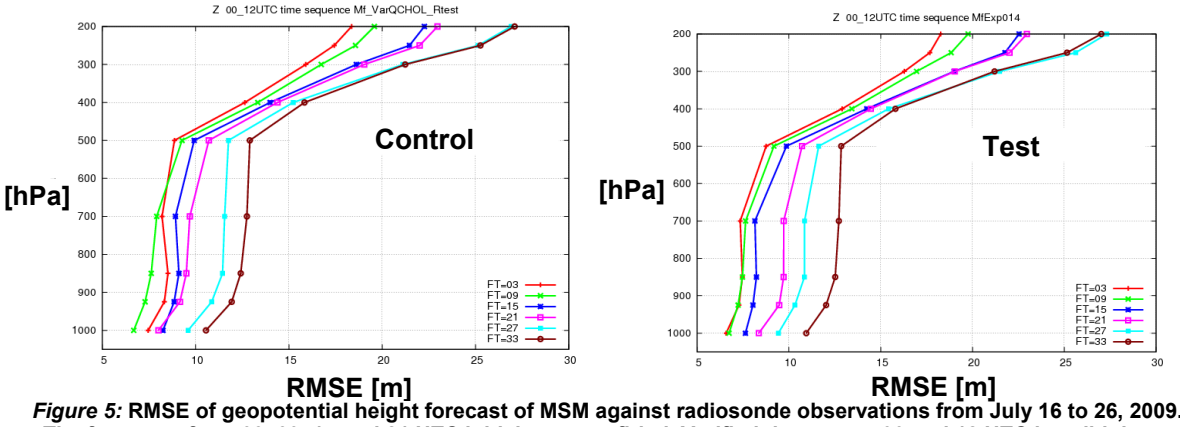

Figure 5: **RMSE of geopotential height forecast of MSM against radiosonde observations from July 16 to 26, 2009. The forecasts from 03, 09, 15 and 21 UTC initials were vefiried. Verified times were 00 and 12 UTC in valid time. The color indicate the difference of Forecast Time (FT). Red (FT=3), Green (FT=9), Blue (FT=15), Pink (FT=21), Light blue (FT=27), Brown (FT=33). The left panels is for Control run and the right panels is for Test run.**

It is expected that direct radiance assimilation would bring improvement of forecast accuracy of geopotential height and temperature profiles in the analyses and short range forecasts. Figure 5 shows RMSE of geopotential height forecast of MSM against radiosonde observations. Note that, in Control run, the RMSE of FT (Forecast Time) =3 (Red line) is larger than that of FT=9 (Green line), whereas the RMSE increases with the forecast time in Test. In Test run, RMSE's improvement in the short range (FT=3) in lower troposphere from 1000 [hPa] to 500 [hPa] is remarkable. The reason of a degradation of the short range forecast accuracy in Control run was thought as imbalanced observation data coverage and amount in the three hourly cycle of the MSM analysis. Use of radiance data along with additions of new satellite's radiance data filled the gap of the observation information. Also it is thought that the direct radiance assimilation of AMSU-A and the use of the radiance data over land (only sensitive channels to higher level atmospheric temperature) mainly contributed the improvement (Kazumori 2010).

As for moisture information, TCWV retrievals from AMSR-E and TMI were assimilated in Control run, whereas AMSR-E and TMI radiance data were assimilated directly in Test run. DMSP F-16, F-17 SSMIS radiance data and MHS data were added and they contain lower and upper tropospheric moisture information, respectively. MTSAT CSR data (Infrared moisture channel) were also incorporated in the analysis. Improvement in the analyzed moisture field and the short range precipitation forecast is expected in Test run.

Figure 6 shows comparison of analyzed TCWV fields between Control run and Test run in 21UTC July 2, 2010 case. There was a stationary front from the continent of China to west part of Japan Islands through East China Sea. A low pressure system was formed on the front in the west part of Japan Sea. In Test run, the analyzed TCWV in East China Sea was larger (about 5 to 10 mm) than that of Control run. Note that moisture flow from southwest around Kyuushu area was strengthened in the Test run and the TCWV exceeded 70 mm.

Figure 7 shows three hour accumulated rainfall for 03UTC July 3, 2010 from some initial times. Upper panels indicate the rainfall forecasts of Control run and middle panels indicate those of Test run. The initial times are 21, 15 and 09 UTC July 2, 2010 from the left side, and they correspond to be 6 hour, 12 hour and 18 hour forecasts, respectively. The lower panel is rainfall distribution from radar observation which is calibrated with rain gauges. Notable change was found in the 6 hour rainfall forecast from 21UTC July 2, 2010 initial (left panels in the upper and middle). Strong rainfall (50 mm/3hour) was predicted around the south of Kyuusyu and Tanegashima Island in Test run, whereas only weak rainfall was predicted for those areas in Control run. Predicted rainfall differences in other forecast ranges were smaller than the 6-hour rainfall forecast difference. The improvement of rainfall forecast was outstanding in the short range forecast. It is likely that the TCWV difference and southwest moisture flow over the ocean shown in Figure 6 brought the rainfall forecast improvement.

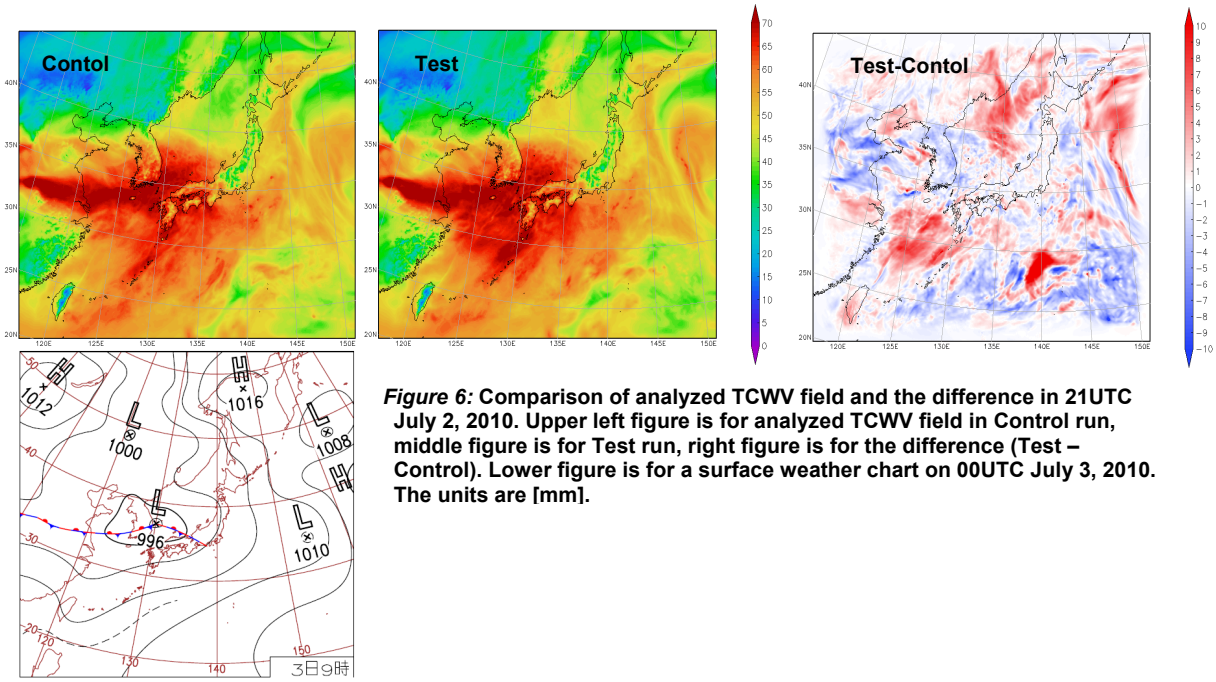

Figure 6: **Comparison of analyzed TCWV field and the difference in 21UTC July 2, 2010. Upper left figure is for analyzed TCWV field in Control run, middle figure is for Test run, right figure is for the difference (Test – Control). Lower figure is for a surface weather chart on 00UTC July 3, 2010. The units are [mm].**

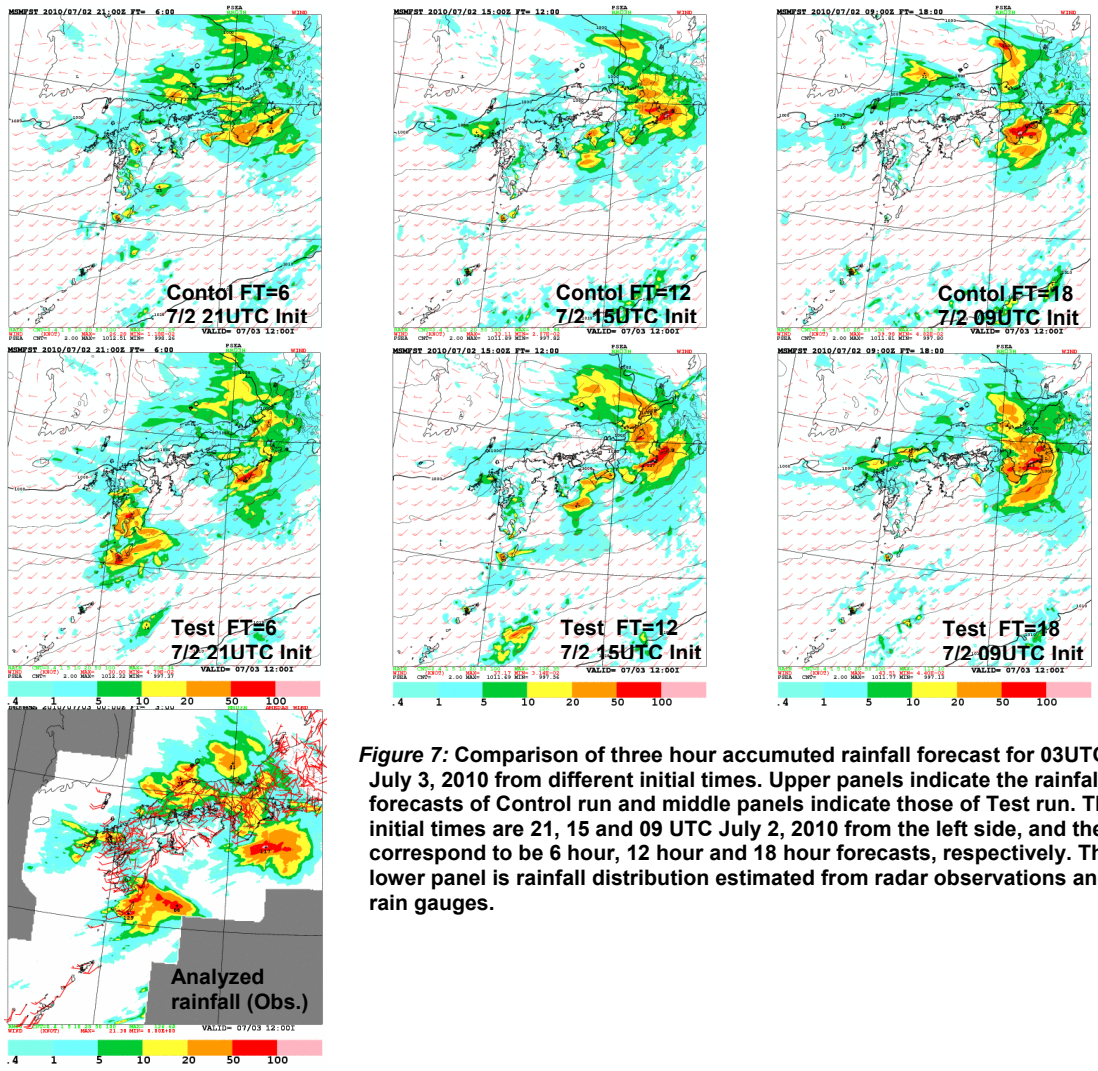

Figure 7: **Comparison of three hour accumuted rainfall forecast for 03UTC July 3, 2010 from different initial times. Upper panels indicate the rainfall forecasts of Control run and middle panels indicate those of Test run. The initial times are 21, 15 and 09 UTC July 2, 2010 from the left side, and they correspond to be 6 hour, 12 hour and 18 hour forecasts, respectively. The lower panel is rainfall distribution estimated from radar observations and rain gauges.**

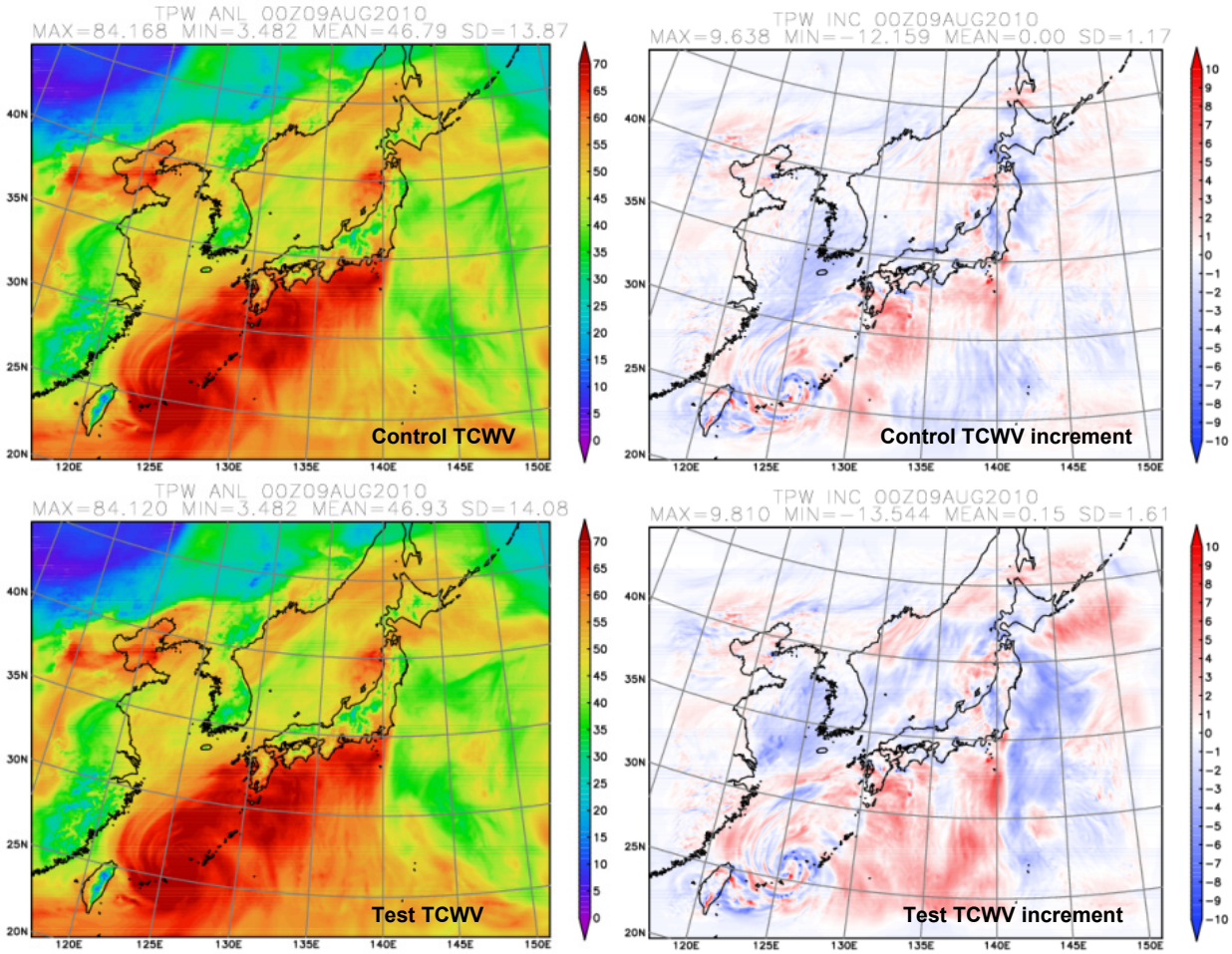

Figure 8: **Comparison of analyzed TCWV field and TCWV analysis increment on 00UTC August 9, 2010 in Test and Control. Left figures indicate analyzed TCWV (Upper: Control run, Lower: Test run). Right figures indicate analysis increment (Upper: Control run, Lower: Test run). The units are [mm].**

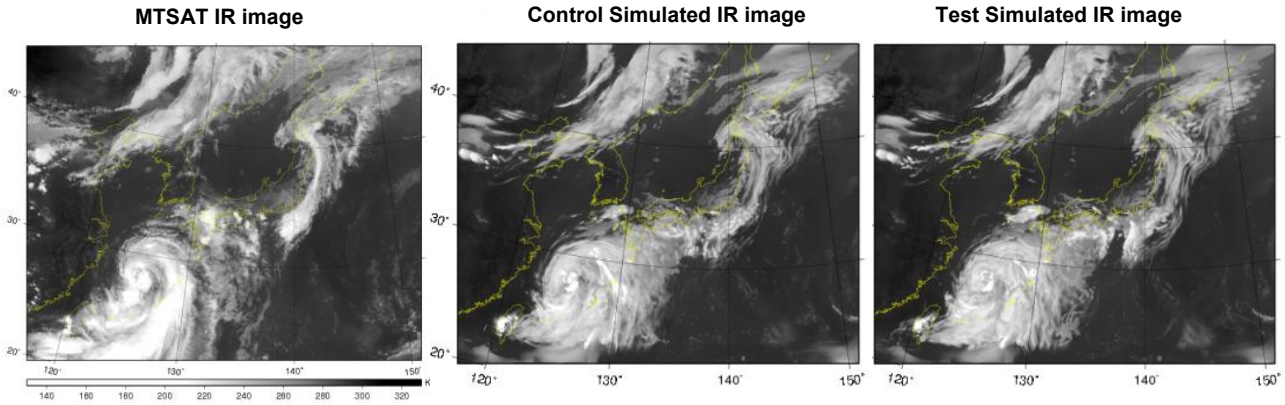

Figure 9: **Comparison of MTSAT's observed IR image and simulated image from MSM analysis field on 09UTC August, 2010. Left panel is for observed IR image, middle panel is for simulated IR image from Control run, right panel is for simulated IR imager from Test run.**

Figure 8 shows comparison of analyzed TCWV field and TCWV analysis increment on 00UTC August 9, 2010 in Test and Control. In this case, subtropical high pressure system was located in the east of Japan Island and the high pressure system was characterized as 30-40 mm TCWV range (Green area), whereas moisture flow along the high pressure edge was described as 50-70mm TCWV range. TCWV analysis increment along Japan Island coast was similar between Test and Control. However, over the ocean, Test run's TCWV analysis imcrement was larger. As GPS TCWV and rain rate from ground-based radar was commonly used in Test and Control, they produced similar increment around

Japan Island. Addition of new Microwave Imagers F-16, F-17 SSMIS increased increment over the ocean and the increment was seamless from the land to the ocean. And the increment in Test run enhanced the TCVW contrast along the edge of the high pressure system.

Figure 9 shows comparison of MTSAT‘s observed IR image and simulated image from MSM analysis field on 09UTC August, 2010. Note that separated cloud feature located in the south of Kantou area was well represented in the Test run. This result suggests that the analyzed tropospheric moisture field of Test run became more realistic than that of Control run.

SUMMARY

Direct radiance assimilation scheme was operationally implemented in JMA meso-scale analysis on 13 December 2010. The assimilation of ATOVS temperature retrievals and TCWV retrievals from Microwave Imagers (AMSR-E, TMI) was ended. Assimilation of AMSU-A, AMSR-E, TMI radiances was started. And new radiance data from DMSP F-16, F-17 SSMIS and MHS onboard NOAA 18, 19 and Metop, CSR from MTSAT were incorporated in the analysis. As the fast radiative transfer model for the forward and adjoint calculation, RTTOV-9.3 was implemented to use same radiance bias correction of JMA global analysis.

Assimilation experiments showed considerable positive impacts on the tropospheric temperature and humidity in the analyses and the short-range forecasts. Reduction of RMSE of geopotential height forecast was confirmed against radiosonde observations. Assimilations of the radiances from various microwave imagers, humidity sounders and MTSAT CSR produced realistic tropospheric moisture field. Simulated MTSAT infrared image from the analysis in the radiance assimilation showed similar features to the real MTSAT image. And improvement of precipitation forecast was also confirmed in the short range forecast.

It was proven that the contribution of satellite data to the analyses and forecast accuracy in JMA meso-scale analysis became larger than previous retrieval assimilation stage. In order to improve precipitation forecast further, early use of new satellite’s radiance data and assimilation of cloud and rain affected radiance are indispensable.

REFERENCES

Honda, Y., M. Nishijima, K. Koizumi, Y. Ohta, K. Tamiya, T. Kawabata and T. Tsuyuki, (2005) A pre-operational variational data assimilation system for a non-hydrostatic model at the Japan Meteorological Agency. Formulation and preliminary results. Quarterly Journal of the Royal Meteorological Society, **131**, Issue 613, pp 3465-3475

JMA, (2007) Appendix to WMO Technical Progress Report on The Global Data-Processing and Forecasting System and Numerical Weather Prediction. Available from http://www.jma.go.jp/jma/jma-eng/jma-center/nwp/outline-nwp/index.htm

Kazumori, M., (2009a) Impact Study of the RTTOV-9 Fast Radiative Transfer Model in the JMA Global 4D-Var Data Assimilation System. CAS/JSC WGNE Res. Activ. Atmos. Oceanic Modell., **39**, pp 1.21-1.22

Kazumori, M., (2009b) The impacts of an Improved Quality Control and Ocean Emissivity Model for Microwave Radiance Assimilation in the JMA Global 4D-Var Data Assimilation System. CAS/JSC WGNE Res. Activ. Atmos. Oceanic Modell., **39**, pp 1.19-1.20

Kazumori, M., (2010) Initial Results of a Direct Radiance Assimilation Experiment in the JMA Mesoscale 4D-Var data assimilation system, CAS/JSC WGNE Res. Activ. Atmos. Oceanic Modell., **40**, 1.19-1.20

Saunders, R. W., (2008) RTTOV-9 Science and Validation Report. EUMETSAT, NWPSAF-MO-TV-020, pp. 74